

Electric Field Computation from Particle Distributions: A Study of Boundary Effects

Yaowaluk Buanill

Suranaree University of Technology, B6211066@g.sut.ac.th

This study examines the influence of boundaries on electric fields arising from uniform and Gaussian particle distributions within accelerators like the SIS100 at FAIR. Initial investigations were conducted without considering boundaries, progressing to scenarios that incorporate boundary considerations. Findings highlight computational challenges in Gaussian distributions and emphasize the importance of symmetrical configurations in bounded settings. The research underscores the necessity for efficient field computation methods in real-world accelerator contexts.

1 Introduction

As the world of particle physics evolves, so do the facilities designed to probe its mysteries. The Facility for Antiproton and Ion Research (FAIR) in Darmstadt, Germany, stands at the forefront of this progress. One of FAIR's promising components, the SIS100 accelerator, highlights the significance of boundaries, like vacuum pipes, in affecting the electric fields generated by charged particle distributions. This study explores how electric fields, originating from both uniform and Gaussian particle distributions, interact with boundaries similar to those in accelerators. Initial investigations considered fields without boundary influences. As the research progressed, the effects of these boundaries were introduced and analyzed. The primary focus of this work is on identifying efficient methods for computing these fields, essential for real-world accelerator applications such as the SIS100.

1.1 Research tools and repository

To lay the groundwork for this study, several essential Python libraries were incorporated. PyPIC[1] serves as a pivotal tool, utilizing the numerical particle-in-cell (PIC) algorithm: given a charge distribution, represented by electric charge density ρ , the algorithm first interpolates onto a regular grid. The potential ϕ is obtained by solving the discrete Poisson equation,

tion,

$$\nabla^2 \phi = -\frac{\rho}{\epsilon_0}, \quad (1)$$

where ∇^2 is the Laplacian operator and ϵ_0 is the electric vacuum permittivity. Within PyPIC, the FFT (Fast Fourier Transform) [6] technique is employed for unbounded charge distributions in free space. On the other hand, the FDSW (Finite Difference with Shortley-Weller) [5] technique is employed for bounded distributions, ensuring the potential at the boundary on the grid approaches zero by modifying the discrete Poisson equation. Hereafter, we will refer to it simply as the Finite Difference (FD) method for brevity. `numpy` is employed for various calculations, spanning mathematical operations to particle generation, while `matplotlib` aids in plotting and data visualization. Following open science and FAIR principles, the entire codebase, results, and a concise overview of the work have been made available via Ref. [2].

1.2 Importance of geometry

In accelerator physics, the importance of geometry is widely recognized. This is highlighted by the elliptical design adopted for the SIS100 ring. A symmetric circular uniform disk was initially investigated, before attention was directed towards the more realistic Gaussian distributions.

2 Free space considerations

In the following analyses without boundary, we denote e as the elementary charge and x and y as the coordinates of the charged particles. For simplicity and to align with typical 2d considerations in accelerator beam dynamics, we assume a uniform linear charge density λ per unit length (i.e., per meter).

2.1 Uniform charge distribution

The electric field produced by a uniform charge distributed within a circular region of radius R centered at $(x, y) = (0, 0)$ along the x-axis was assessed. This was done using both the Fast Fourier Transform (FFT) method from the PyPIC library and an analytical approach rooted in Gauss's law. The resulting equation from Gauss's law, which describes the electric field in terms of λ and R , is:

$$E_{x_{\text{circ}}} = \begin{cases} \frac{\lambda}{2\pi\epsilon_0} \frac{x}{R^2} & |x| \leq R \\ \frac{\lambda}{2\pi\epsilon_0} \frac{1}{x} & |x| \geq R \end{cases} \quad (2)$$

The electric field, computed along $y = 0$ (x-axis), demonstrates consistent results between the analytical approach given by Eq. (2) and the numerical method, FFT. This congruence can be observed in Fig. 1, where the fields from both methods overlap. Adjacent to this representation in the same figure, the circular uniform distribution with a radius of 0.02 m is depicted on the right side.

2.2 Round Gaussian charge distribution

The electric field arising from a Gaussian charge distribution centered at $(x, y) = (0, 0)$ amounts to

$$E_{x_{\text{Gauss}}} = -\frac{\lambda}{4\pi\epsilon_0} \times x \times \int_0^\infty \frac{\exp\left(-\frac{x^2}{2\sigma_x^2+t} - \frac{y^2}{2\sigma_y^2+t}\right)}{(\sigma_x^2+t)\sqrt{(\sigma_x^2+t)(\sigma_y^2+t)}} dt \quad (3)$$

where σ_x and σ_y represent the standard deviations for the respective plane. For the round case, the standard deviation of this Gaussian distribution is set equal to the one of the uniform distribution, namely $\sigma_{x,y} = R/2$, which corresponds to 0.01 m.

To compute the discrete electric field, we employed the PyPIC library and its associated FFT method, similarly to the approach in section 2.1. For the analytical approach, Eq. (3) provides a direct method; however, the numerical evaluation of this intricate integral is computationally expensive. For the round beam case, the integral can be solved analytically [4]:

$$E_{x_{\text{Gauss}}} = \frac{\lambda}{2\pi\epsilon_0 r^2} \cdot x \cdot \left(1 - \exp\left(-\frac{r^2}{2\sigma^2}\right)\right) \quad (4)$$

where $r^2 = x^2 + y^2$, and σ denotes the standard deviation of the Gaussian distribution.

The electric fields derived from Eq. (4) and those computed using the FFT method show strong agreement. Figure 2 presents these fields alongside those from the linearized version of Eq. (4) and a uniform distribution. Notably, near the center of the distribution, the slope of the Gaussian field is twice as steep compared to the uniform distribution, while both approach the same electric field at large amplitudes. The geometry of the Gaussian charge distribution is also depicted on the right side of the figure.

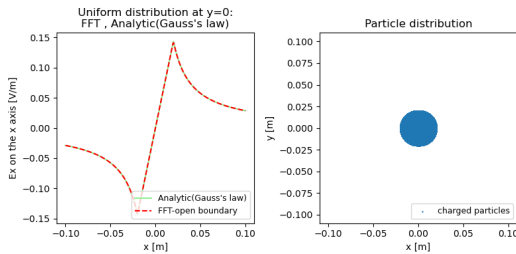


Fig. 1: Electric field along the x-axis due to a uniform charge distribution, and the geometry of the distribution

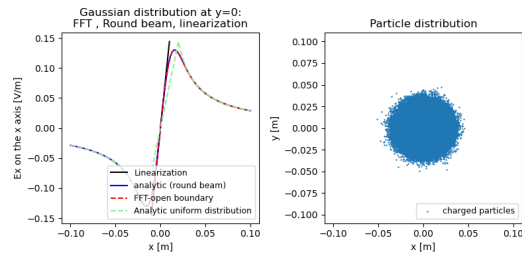


Fig. 2: Electric field along the x-axis due to a round Gaussian charge distribution, and the geometry of the distribution

2.3 Asymmetric elliptic Gaussian charge distribution and Bassetti-Erskine formula

In the case of non-round elliptical Gaussian charge distribution centered at $(x, y) = (0, 0)$, the equation for the electric field of a round beam (given by equation 4) becomes inapplicable. An alternative approach would be to use the integral form of the Gaussian distribution, as represented by Eq. (3). However, this method can be computationally intensive. The Bassetti-Erskine method [7], which leverages the Faddeeva function,

$$w(z) = \exp(-z^2) \left[1 + \frac{2i}{\sqrt{\pi}} \int_0^z e^{t^2} dt \right], \quad (5)$$

offers a more computationally efficient electric field expression¹.

For the Bassetti-Erskine formula to be valid, the standard deviations must differ, $\sigma_x \neq \sigma_y$. Here, we consider $\sigma_x = 1.5\sigma_y$ with $\sigma_y = R/2$ set to 0.01 m. The computational region for the FFT method is expanded accordingly to be 1.5 times larger in the x-plane compared to the y-plane, creating an asymmetric computational domain for the FFT.

Comparing the electric fields calculated using both the semi-analytic Bassetti-Erskine equation and the numerical FFT method reveals matching results for the elliptic Gaussian distribution, as depicted in Fig. 3. Furthermore, by referencing the results from Eq. (4) computed using a round beam (from Fig. 2), it becomes evident that Eq. (4) is not suitable for the case of an elliptical charge distribution where σ_x differs from σ_y .

3 Boundary Considerations

In accelerators, the beams are confined in a vacuum pipe. The effect particularly of the SIS100 vacuum pipe on the electric field of the distribution is to be investigated. While studies have been conducted on the SIS100 [3], the influence of the boundary has not been extensively explored, making this study's focus especially pertinent. For a more accurate simu-

¹ The Bassetti-Erskine expression reads

$$E_y + iE_x = -\frac{\lambda}{2\epsilon_0 \sqrt{2\pi(\sigma_x^2 - \sigma_y^2)}} \left[w\left(\frac{x + iy}{\sqrt{2(\sigma_x^2 - \sigma_y^2)}}\right) - \exp\left(-\frac{x^2}{2\sigma_x^2} - \frac{y^2}{2\sigma_y^2}\right) w\left(\frac{x\left(\frac{\sigma_y}{\sigma_x}\right) + iy\left(\frac{\sigma_x}{\sigma_y}\right)}{\sqrt{2(\sigma_x^2 - \sigma_y^2)}}\right) \right]$$

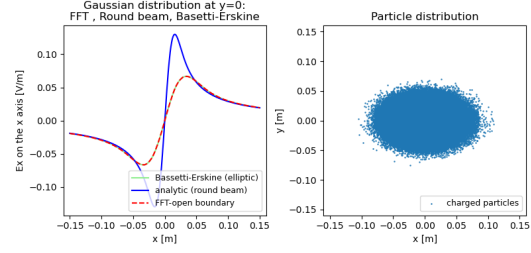


Fig. 3: Electric field along the x-axis from a Gaussian distribution in an ellipse shape is compared to the one from a circular shape, and the geometry of the ellipse shape distribution

lation of such environments, it is essential to account for these boundaries. One approach to achieving this is by solving the Poisson equation with the stipulation that the potential is set to zero at the boundary. The electric field of the beam is thus distorted to be perpendicular to the boundary. The Finite Difference with Shortley-Weller (FDSW) method, here abbreviated as the Finite Difference (FD) method, available in the PyPIC package, is well-suited for this task. While a symmetric boundary around a symmetrically located distribution has no impact on the electric field, asymmetric boundaries or dislocated distributions can lead to substantial distortions. For simulating these different scenarios and demonstrating the distortion, the FFT method is employed as a proxy for the open boundary case, while the FD method gives the correct result for a closed boundary. Here, we consider round beams in a round pipe.

3.1 Uniform Charge Distribution

For the uniform charge distribution, we retain the parameters previously defined in the unbounded scenario. The distribution has a set radius of $R = 0.02$ m, and the vacuum pipe, serving as the boundary, has a radius of 0.1 m. The charge distribution remains centrally positioned at $(x, y) = (0, 0)$.

The simulation results for this setup, along with the accompanying geometry of the distribution on the right side, are illustrated in Fig. 4. Both FFT and FD results are congruent, which is

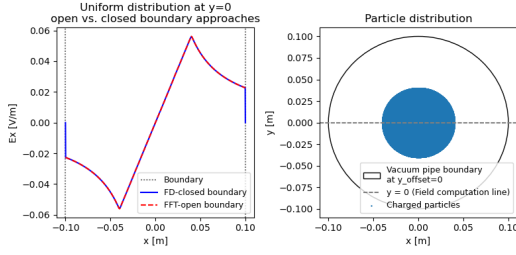


Fig. 4: Electric field along the x -axis due to a uniform charge distribution with boundary and the geometry of the distribution

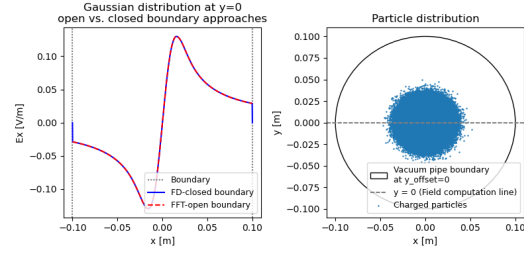


Fig. 6: Electric field along the x -axis due to a Gaussian charge distribution with boundary and the geometry of the distribution

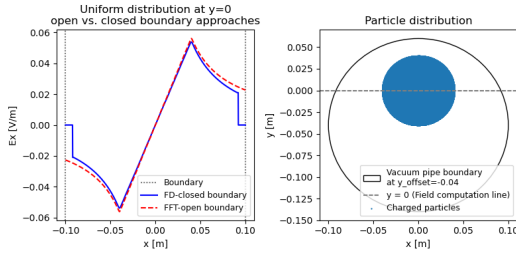


Fig. 5: Electric field along the x -axis due to a uniform charge distribution with boundary with offset = -0.04 m and the geometry of the distribution

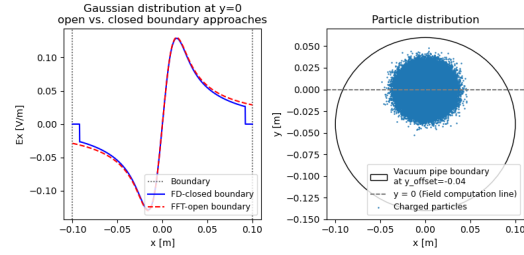


Fig. 7: Electric field along the x -axis due to a Gaussian charge distribution with boundary with offset = -0.04 m and the geometry of the distribution

expected given the symmetric arrangement of the charge distribution inside the vacuum pipe.

Upon altering the chamber's position downward to $y = -0.04$ m, this symmetry is broken. The resulting disparity between the FFT and FD methods is evident in Fig. 5. This discrepancy primarily emerges due to the asymmetry introduced by shifting the vacuum pipe.

3.2 Gaussian Charge Distribution

For the Gaussian charge distribution, we again adhere to the parameters set in the unbounded context. Retaining these specifications, the charge distribution is centered at $(x, y) = (0, 0)$.

Results from our simulations, using these parameters, are showcased in Fig. 6. As with the uniform distribution, there is an agreement between the FFT and FD computations due to the symmetric placement of the charge within the vacuum pipe.

Introducing asymmetry by adjusting the chamber's position to $y = -0.04$ m leads to variations between the FFT and FD results, as displayed in Fig. 7. Similar to the uniform distribution, this difference is attributed to the distortion of symmetry caused by the chamber's displacement.

4 Conclusion

For unbounded cases, we compared analytical equations to the numerical FFT method. Uniform charge distributions proved straightforward, while Gaussian distributions presented computational challenges due to the intricate integral equation involved. For round distributions ($\sigma_x = \sigma_y$), the analytic formula yielded consistency with FFT results. For elliptical distributions ($\sigma_x \neq \sigma_y$), the semi-analytic Bassetti-Erskine approach preserved this consistency.

Shifting to bounded scenarios with a vacuum pipe, centered charge placements mirrored unbounded results. However, deviating from this symmetry—by repositioning the pipe—revealed the expected discrepancies between FD and FFT calculations due to the distortion of the electric field by the present boundary.

5 Outlook

One key takeaway from our studies is that while the FD method is thorough, it is also computationally expensive. Therefore, future endeavors could focus on deriving a semi-analytical formula akin to the Bassetti-Erskine formulation but tailored to include the boundary effect.

Acknowledgments

The author wishes to offer profound and heartfelt gratitude to Adrian Oeftiger. His continuous support and extensive knowledge, ranging from beam dynamics to programming to how to learn, have been not only instructional but transformative.

Furthermore, my gratitude is extended to GSI for offering the opportunity to embark on this journey as a summer student. This project was a good learning experience, and the assistance and tools offered by GSI were critical in its completion.

References

- [1] Iadarola, G., Oeftiger, A., et al. (2023). PIC codes at CERN, software repository, PyCOMPLETE/PyPIC. url: <https://github.com/PyCOMPLETE/PyPIC>
- [2] Buanill, Y. (2023), Zenodo software repository, YaowalukB/indirect-beam. url: <https://doi.org/10.5281/zenodo.8322384>
- [3] Oeftiger, A., Boine-Frankenheim, O., Chetvertkova, V., Kornilov, V., Rabusov, D. and Sorge, S. (2022). *Simulation study of the space charge limit in heavy-ion synchrotrons*. Phys. Rev. Accel. Beams, 25, 054402, <https://link.aps.org/doi/10.1103/PhysRevAccelBeams.25.05440>
- [4] Herr, W. (2006). *Beam-beam interactions*. url: <https://cds.cern.ch/record/941319>
- [5] Shortley, G., & Weller, R. (1938). *The numerical solution of Laplace's equation*. Journal of Applied Physics, 9(6), 334-348.
- [6] Cooley, J. W., & Tukey, J. W. (1965). *An algorithm for the machine calculation of complex Fourier series*. Mathematics of computation, 19(90), 297-301.
- [7] Bassetti, M. & Erskine, G. (1980). *Closed expression for the electrical field of a two-dimensional Gaussian charge*. url: <https://cds.cern.ch/record/122227>